Environ Monit Assess (2020) 192: 568
https://doi.org/10.1007/s10661-020-08493-x

Impacts of industrial atmospheric emissions on watershed export of dissolved ions in coastal streams: a Bayesian modeling approach

Timothy J. Maguire · **R. Paul Weidman** ·
Scott O. C. Mundle · **Jonathan W. Moore** ·
Kyle A. Chezik · **Daniel T. Selbie**

Received: 29 January 2020 / Accepted: 13 July 2020

Abstract Anthropogenic atmospheric emission and subsequent deposition of sulfur (S) has been linked to disrupted watershed biogeochemical processes through soil and surface water acidification. We investigated watershed-scale impacts of acidic deposition on tributary concentrations and watershed exports of major nutrients and ions for the Kitimat River Watershed, British Columbia. Since the 1950s, the Kitimat watershed had an aluminum smelting facility with substantial emissions at the river estuary. Emissions load the airshed overlying the watershed and potentially impact western tributaries leaving eastern tributaries available as reference. We assessed concentrations and export of key compounds in three reference and six potentially impacted tributaries and watersheds in 2015 and 2016. Sulfate (SO_4), fluoride (F), nitrate (NO_3), and chloride (Cl) were significantly higher in impacted tributaries. F concentrations exceeded the Canadian Council of Ministers of the Environment guideline for aquatic life in 83% of samples collected from impacted streams. Watershed export and associated uncertainty were determined by bootstrapped flow-stratified Beale's unbiased estimator. Impact of emissions on watershed export was modeled in a Bayesian approach to include variance in the export estimate to inform the uncertainty of model parameters. Export of SO_4 and Ca increased significantly within 16 km and 8 km, respectively, toward the smelter emissions. The corresponding impacted area for SO_4 and Ca was approximately 100 km^2 and 45 km^2, respectively. SO_4 export is likely due to direct impacts of S deposition, with excess S being flushed from the watersheds. Ca export patterns likely result from indirect impacts of S deposition on soil chemistry and flushing of Ca. These impacts may contribute to effects within tributaries on benthic stream communities and regionally important juvenile Pacific salmon.

Keywords Watersheds · Streams · Atmospheric deposition · Sulfur · Nitrogen · Calcium · Salmon

Electronic supplementary material The online version of this article (https://doi.org/10.1007/s10661-020-08493-x) contains supplementary material, which is available to authorized users.

T. J. Maguire (✉) · R. P. Weidman · S. O. C. Mundle
Great Lakes Institute for Environmental Research, University of Windsor, Windsor, ON, Canada
e-mail: maguiret@uwindsor.ca

R. P. Weidman · J. W. Moore · D. T. Selbie
School of Resources and Environmental Management, Simon Fraser University, Burnaby, BC, Canada

S. O. C. Mundle
Department of Chemistry and Biochemistry, University of Windsor, Windsor, ON, Canada

J. W. Moore · K. A. Chezik
Earth to Oceans Research Group, Simon Fraser University, Burnaby, BC, Canada

D. T. Selbie
Fisheries and Oceans Canada, Science Branch, Pacific Region, Cultus Lake Salmon Research Laboratory, Cultus Lake, BC, Canada

Introduction

Human activities increase atmospheric emissions of sulfur (S) via fossil fuel combustion in power plants, smelters, and oil and gas operations (McLinden et al. 2016). These atmospheric emissions have been linked to many deleterious ecological effects. Large regional emissions and deposition of S have been linked with soil and surface water acidification, mobilization of toxic soil components, such as aluminum (Al) or strontium (Sr), and depletion of cations, namely calcium (Ca), via changes in soil cation exchange (Likens et al. 1996a, b; Mitchell et al. 2011; April et al. 2016). Sulfate (SO_4) concentrations in mesocosms have shown increases in the release of toxic methylmercury due to microbial sulfate reduction (Myrbo et al. 2017). Cumulatively, these impacts disrupt watershed biogeochemical processes.

Some processes buffer the negative effects of S emissions, including geological weathering rates and acid buffering capacity of soil and water. S deposited on forests can be incorporated into forest floor organic materials (Prietzel et al. 2004). Wetlands can incorporate abiotic S into dissolved organic matter (Sleighter et al. 2014), which results in the formation of iron sulfide and hydrogen sulfide gas. Iron sulfide may later remobilize sulfur, whereas hydrogen sulfide is lost from the watershed (Reddy and DeLaune 2008). Accumulated S within watersheds may be retained until the emission source is removed and precipitation leaches the remaining S, depending on S adsorption capacity of soil (Rice et al. 2014). Accumulation of anthropogenic sulfur in soil may result in forest floor acidification, depletion of exchangeable nutrient cation pools, increased podzolization, and reduced nitrogen (N) availability for trees if deposition exceeds the acid buffering capacity (Prietzel et al. 2004). The effects of acid precipitation and deposition on soils eventually impact watershed export of nutrients. Rivers are primary delivery pathways for biologically available N, phosphorus (P), and silica (SiO_2) to the ocean (Meybeck 1982; Schlesinger and Bernhardt 2013; Tréguer and De La Rocha 2013). Primary producers require available nutrients in prescribed ratios, if one nutrient is lagging, it can become limiting for growth (Redfield 1958). Thus, changes to nutrient delivery caused by anthropogenic atmospheric emissions can have far-reaching repercussions across downgradient trophic levels.

The ecological consequences of acidic deposition on forested watersheds in British Columbia, Canada, have been investigated previously in the Kitimat River watershed. Since the 1950s, an aluminum smelter located at the river estuary has been a large emission source of atmospheric S. Recently, a major upgrade ($6 billion) to the smelter increased emissions of S but decreased emissions of fluoride (F) gas (Rio Tinto 2018). Previous studies of the Kitimat River watershed have estimated spatial deposition patterns of S (ESSA Technologies et al. 2013, 2014, 2019; Cowden and Aherne 2019), modeled impacts on acid buffering capacity of soils (Williston et al. 2016), and observed impacts on terrestrial vegetation (Bunce 1989). However, to date, studies have not quantified watershed-level impacts on small tributaries within the Kitimat watershed, important habitats for Pacific salmonids, such as the S-mediated export of biologically important nutrients. Moreover, nutrient export is a challenge to accurately estimate in reaches where concentration data are sparse, even if flow data are available. However, stratifying export methodologies by flow and using Bayesian frameworks can overcome these challenges. The objective of this study was to quantify watershed-scale impacts of acidic deposition on watershed processes and export of S, N, and other major nutrients and ions in the Kitimat River watershed, within the traditional territory of the Haisla First Nation, on the North Coast of British Columbia, to estimate the impact of emissions on exports and delineate spatial extent of impacts. In this region of British Columbia, proposed and in-construction multi-billion dollar liquefied natural gas (LNG) export facilities would further increase emission and deposition of atmospheric S and N due to the combustion of large amounts of natural gas involved in the export process (Williston et al. 2016). These facilities create a pressing need to quantify current anthropogenic watershed impacts, such that cumulative effects of additional loadings can be quantified and associated ecological impacts assessed (Williston et al. 2016).

Methods

The Kitimat River is located at the North Coast of British Columbia within a 90 km by 12 km valley running north-south (Fig. 1) (Williston et al. 2016). The valley is divided with small tributaries draining eastern and western watersheds. Watersheds are mostly forested, have been previously logged, are subject to forestry management plans aimed to reduce soil ion loss, and contain very little commercial agriculture (Rabnett 2014; Williston et al. 2016). There is a 60-year legacy of atmospheric deposition of S from the Rio Tinto Alcan (RTA) aluminum smelter, which is located near the Haisla First Nation Village of Kitamaat (N 53.9749°, W 128.6490°), and near the town of Kitimat (N 54.0547°, W 128.6580°). Currently,

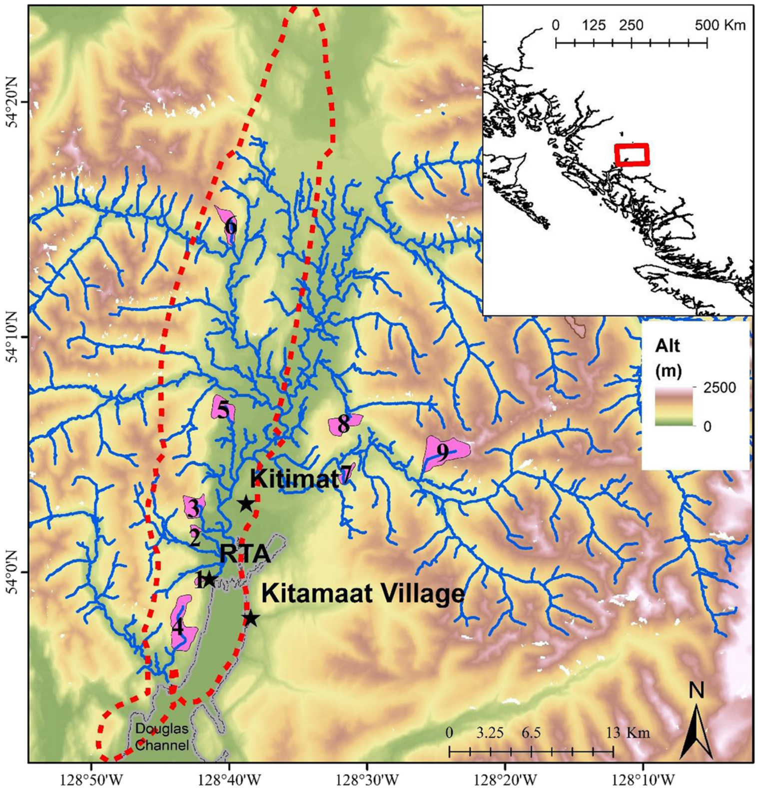

Fig. 1 The study area was comprised of 9 sub-watersheds (pink polygons) throughout the Kitimat River watershed. For more than 50 years, atmospheric deposition of S from the Rio Tinto Alcan (RTA) aluminum smelter has impacted the western sub-watersheds, leaving the eastern sub-watersheds as reference. The red dashed line represents an area of 210 km^2 where background/natural S deposition (assumed to be ≤ 9 kg total SO_4 ha^{-1} y^{-1}) (Vet et al. 2014) is doubled due to emissions from the smelter; this was calculated using 30-year average annual emissions from the smelter of 19 tons sulfur dioxide day^{-1} ± 2.8 SD) (ESSA Technologies et al. 2013). There are two populations adjacent to the smelter; the town of Kitimat is located northeast, while the Haisla First Nation Kitamaat Village is located southwest across the Douglas Channel. Watershed are numbered with increased distance from the smelter (Appendix A, Table S1 and S2).

atmospheric emissions from the smelter are dominated by sulfur dioxide (SO_2; ~ 30 tons SO_2 day^{-1}), but also include nitrogen oxides (NO_x; ~ 1 ton NO_x y^{-1}) and gaseous fluoride (F; ~ 0.4 tons F y^{-1}) (Williston et al. 2016; Rio Tinto 2018). Atmospheric emissions from the smelter were reduced in 2015, but increased in 2016 after the smelter upgrade (Rio Tinto 2018), although our study was focused on investigating effects of long-term atmospheric deposition and not interannual differences. Previous atmospheric modeling and accompanying confirmatory deposition samples from across the Kitimat watershed have indicated that prevailing wind patterns and topography focus S emissions and deposition toward the western watersheds (Williston et al. 2016). Thus, in our study, we used watersheds on the eastern side of the valley as reference sites. From 1982–2011, average SO_2 emissions from the smelter were 19 tons SO_2 day^{-1} ± 2.8 SD (ESSA Technologies et al. 2013). As a result, atmospheric S deposition was doubled over an area of 210 km^2 in the western Kitimat watershed (Fig. 1), relative to background total S deposition that was previously estimated to be ~ 3 kg total S ha^{-1} y^{-1} (ESSA Technologies et al. 2014; Vet et al. 2014). This area was calculated using 30-year average annual emissions from the smelter of 19 tons SO_2 day^{-1} ± 2.8 SD (ESSA Technologies et al. 2013; 2014). There were no systematic differences in the underlying geology between reference and impacted locations (i.e., exposed to industrial atmospheric deposition). Bedrock geology of the study sites is defined as quartz dioritic intrusive bedrock (Fig. 1; impacted sites # 1, 4, and 6; reference sites # 7, 8, and 9) and calcareous-alkaline volcanic bedrock (Fig. 1; impacted sites # 2, 3, and 5) (ESSA Technologies et al. 2013).

Samples were collected from July to December in 2015 and 2016 approximately weekly from 9 tributary watersheds, including 3 watersheds located on the reference side of the valley (Fig. 1). Stream water samples (*n* = 225) were collected in prewashed polyethylene bottles, filtered with 0.45 μm GFF filters, shipped frozen to the Cultus Lake Salmon Research Laboratory (Fisheries and Oceans Canada (DFO), Cultus Lake, BC), where samples were stored frozen until analysis. Dissolved SO_4, nitrate (NO_3), Ca, magnesium (Mg), chloride (Cl), sodium (Na), and fluoride (F) were analyzed using a capillary ion chromatography instrument (Dionex, ICS-5000) with dual anion/cation columns (Appendix A Table S1). Concentrations were calculated using external reference standards (Dionex, anion/cation standards mixture II). Prior to analysis, samples were thawed at 4 °C for 24 hours, transferred into sampling vials and injected directly into the instrument. Samples were analyzed in duplicate to ensure quality control. Because the data were not normally distributed, differences between impacted and reference tributary concentrations were tested with the non-parametric Wilcoxon rank sum test.

Stream water levels at the nine study sites were measured continuously in summer and fall using water pressure loggers (Solinist Canada Ltd., model "level logger edge") located in plastic wells installed in the stream bed. Stream water levels were adjusted for barometric changes measured using atmospheric pressure sensors (Solinist Canada Ltd., model "barologger edge"), which were installed at three study sites roughly 15 km apart. At site # 4 (Renegade Creek), barometric-adjusted stream level was also measured continuously throughout the entire year at a permanent hydrological station operated by Environment Canada. Daily stream level for each study site was calculated over the entire year using stream level data from the permanent hydrological station. Daily discharge was measured monthly at the nine study sites with a current meter (Swaffer Instruments Inc., model 2100). Rating curves were constructed based on stream level and observed discharge to estimate unobserved flow values (CABIN 2012).

Mean seasonal export of SO_4, NO_3, Ca, Mg, Cl, Na, and F were estimated for each of the 9 main study streams using data from 2015 to 2016. Seasonal export was limited to summer (July–September) and fall (October–December). Export was estimated with Beale's unbiased estimator (Beale 1962; Dolan et al. 1981), which has been shown effective in streams with dynamic hydrographs and limited concentration data (Carey and Fulweiler 2013; Fulweiler and Nixon 2005; Maguire and Fulweiler 2017). Within the Beale's estimator, *x* and *y* represent flow and export, $\widetilde{\mu}_y$ is the daily export, μ_x is the mean daily flow for the season, m_y is the mean daily observed export, m_x is the mean daily flow for days with concentration samples collected, *n* is the number of concentration sampling days, S_{xy} is the covariance of daily flow and export, and S_{x^2} is the covariance of flow on concentration sampling days (Eq. 1). The data were stratified by flow into all possible permutations which included a minimum of three concentration samples in each stratum. Uncertainty about each export estimate was determined via bootstrapping with replacement (*n* = 200). The strata scheme which generated an export estimate that was unimodal and had the smallest standard deviation was selected as the best representation of mean seasonal export for each analyte; accordingly, watersheds with fewer samples will generate larger uncertainties about export estimates (Appendix A Table S2) (Maguire and Fulweiler 2017). Export was normalized by the watershed size to estimate a mean seasonal flux (mass km^{-2} season^{-1}; i.e., per 3-month season).

$$\widetilde{\mu}_y = \mu_x \frac{m_y}{m_x} \left(\frac{\left(1 + \frac{1}{n} \frac{Sxy}{m_x m_y}\right)}{\left(1 + \frac{1}{n} \frac{S_{x^2}}{m_{x^2}}\right)} \right) \tag{1}$$

Mean seasonal fluxes from the six watersheds (no fall samples were collected for site # 1; *n* = 11) on the western side of the study area valley were modeled as a function of linear distance from the smokestack (N 54.0003°, W 128.6992°) of the aluminum smelter to the sample collection sites. Models were created as generalized linear mixed effects (GLM) using a gamma distribution and log-link function (Bates et al. 2015). Models of each analyte mean export were generated using a combination of physical descriptors defined in ArcMap (version 10.6.1), distance (fixed effect) and individual watershed, flow path length, and slope (random effects). Random effects were sequentially removed and model selection was conducted via Akaike Information Criterion (AIC) (Bozdogan 1987; Johnson and Omland 2004).

Analytes that were significantly predicted by GLMs as a function of distance were built into a Bayesian model framework. The complete sets of 11 seasonal 200-bootstrapped export estimates were used as response variables to fit a generalized Bayesian linear model with log-link to incorporate the uncertainty of analyte export into estimates of the model coefficients. Using a Bayesian methodology is computationally intense but allows the uncertainty in the export estimate to inform the model parameters instead of the more common approach of using mean export values as response variables. Using this methodology, which incorporates not only the uncertainty in the relationship between export and distance but also the uncertainty in the export estimates themselves, lends confidence to any observed patterns. Uninformed priors and a normally distributed data model were used for the response variable. The resulting Bayesian model of export as a function of distance was compared with the median export values of three watersheds on the eastern side of the valley to establish a radius of impact for affected analytes.

Results and discussion

Concentrations of many compounds were higher in impacted tributaries compared with reference sites (Appendix A Table S1). Significant differences were observed between impacted and reference tributary concentrations of SO_4, F, NO_3, Cl, and Ca (all $p < 0.001$; Fig. 2a and b). Na and Mg concentrations were not significantly different ($p = 0.13$ and $p = 0.68$, respectively). Those analytes which were significantly different had higher values in the impacted tributaries. SO_4 export and Ca export were elevated in catchments # 1–4 and # 1, 3, and 4, respectively, which were underlain by both major geological types in our study area (Fig. 1). F concentrations were also elevated in impacted catchments located on both major geological types. Thus, elevated SO_4, Ca, and F were attributed to industrial atmospheric deposition and not geological differences among sites. Of those analytes with elevated concentrations in impacted tributaries, F concentrations exceeded the Canadian Council of Ministers of the Environment (CCME) guideline for aquatic life (0.12 mg L^{-1}). Exceedances were observed in 83% (148 out of 179) of samples collected. F concentrations did not exceed the CCME guideline for aquatic life in any sample taken from the reference sites. From 2008–2018, average gaseous F emissions from the smelter (344 tons F $year^{-1}$ ± 171 SD) declined from ~ 625 to ~ 175 ton F $year^{-1}$ after the smelter upgrade (Rio Tinto 2018). The likely source of elevated F in the impacted watersheds was industrial atmospheric emissions as impacted watersheds are on both major bedrock types and F was reported within the smelter air plume.

Export was used to estimate the relationship of impact with distance from the smelter because of the different flow conditions and catchment characteristics in each tributary and watershed. Mean seasonal exports were generated for the 9 study streams (Appendix A Table S2, Fig. 3).

SO_4 and Ca export increased significantly with proximity toward the smokestack (SO_4 $p = 0.04$; Ca $p = 0.05$). The best fitting GLM included distance as a fixed effect without random effects for either analyte. SO_4 varied from 0.07 to 5.34 tons km^{-2} $season^{-1}$, while Ca varied from 0.26 to 11.4 tons km^{-2} $season^{-1}$. Our SO_4 and Ca estimates are high in comparison with the available data from watersheds in British Columbia and resemble eastern North America watersheds which have been subject to acidic deposition and tree harvest (Federer et al. 1989). The Bayesian models (Fig. 3) for SO_4 and Ca estimate the distance from the smokestack of the smelter to where exports return to reference conditions to be 16 km (95% CI between 14 and 18 km) and 8 km (95% CI between 6 and 10 km), respectively.

The decrease in SO_4 export with distance from the smelter smokestack indicates the direct impact of S deposition on study area watersheds. The elevated exports of SO_4 in tributaries in proximity to the smokestack are evidence that anthropogenic atmospheric deposition of S is in excess of biological demand and storage, and causes increased stream export from watersheds (Ohrui and Mitchell 1997). Watershed soils adjacent to the smelter emissions could be impacted by acid rain and/or acidic dry deposition if the acid buffering capacity of soils is exceeded. SO_4 export was 4× higher than fluxes reported for southwestern British Columbia (Feller 2010). The 16 km impact distance corresponds to modeled estimates of S deposition of ≥ 24 kg SO_4 ha^{-1} y^{-1} over the past 30 years (Williston et al. 2016), which represents an area of 100 km^2 (Fig. 1).

The impact of acidic deposition on Ca is indirect, and export patterns suggest altered soil chemistry and eventual flushing of Ca from soil water. The pattern in base cation export supports this interpretation. When exposed to acid precipitation, soil cation exchange capacity is altered and Al^{+3} dissolves into solution (pH < 4.7) and subsequently replaces Ca in the soil matrix, causing acid-impacted watersheds to export Ca (Likens et al. 1996a, b). Depleted Ca conditions in lakes in Canada have altered zooplankton communities and impacted food webs (Jeziorski et al. 2015; Yan et al. 1989). Some tributaries of this study area might experience similar ecological shifts if continued or increased acidic deposition denudes the watersheds of Ca beyond the capacity of geological weathering rates to replace Ca in the soil matrix (Reid and Watmough

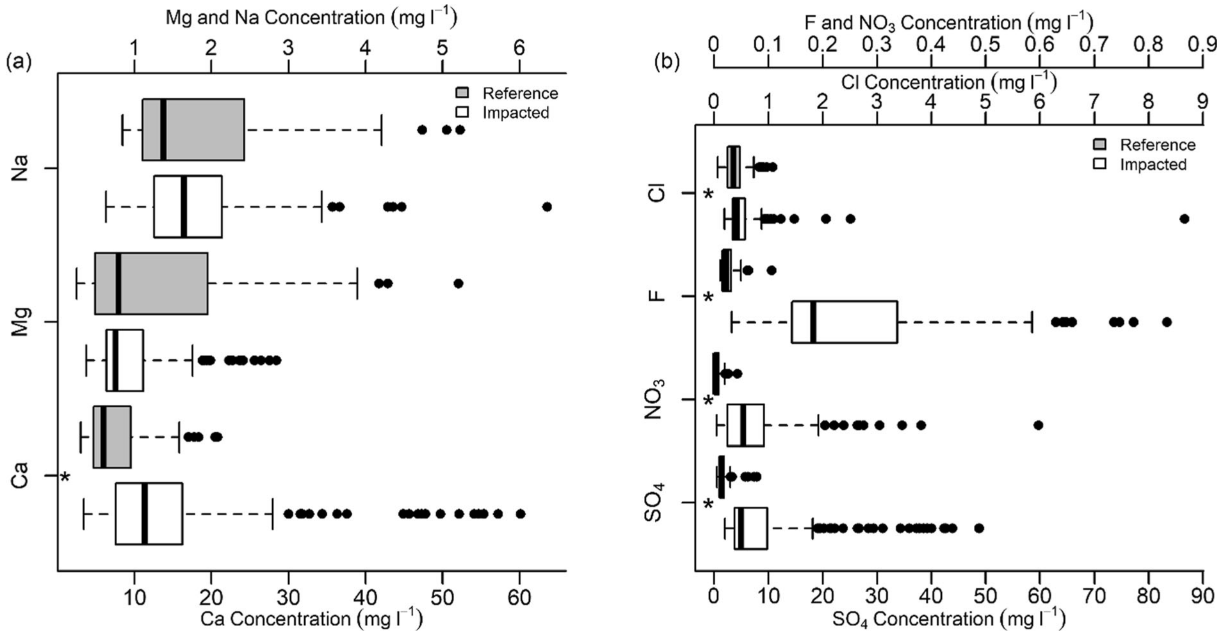

Fig. 2. **a** Concentrations of sodium (Na) and magnesium (Mg) were not significantly different between impacted and reference tributaries; however, calcium (Ca) concentration differences were significant ($p < 0.001$; marked with "*"). **b** Concentrations of chloride (Cl), fluoride (F), nitrate (NO_3), and sulfate (SO_4) were significantly different ($p < 0.001$; marked with "*") between impacted and reference watersheds

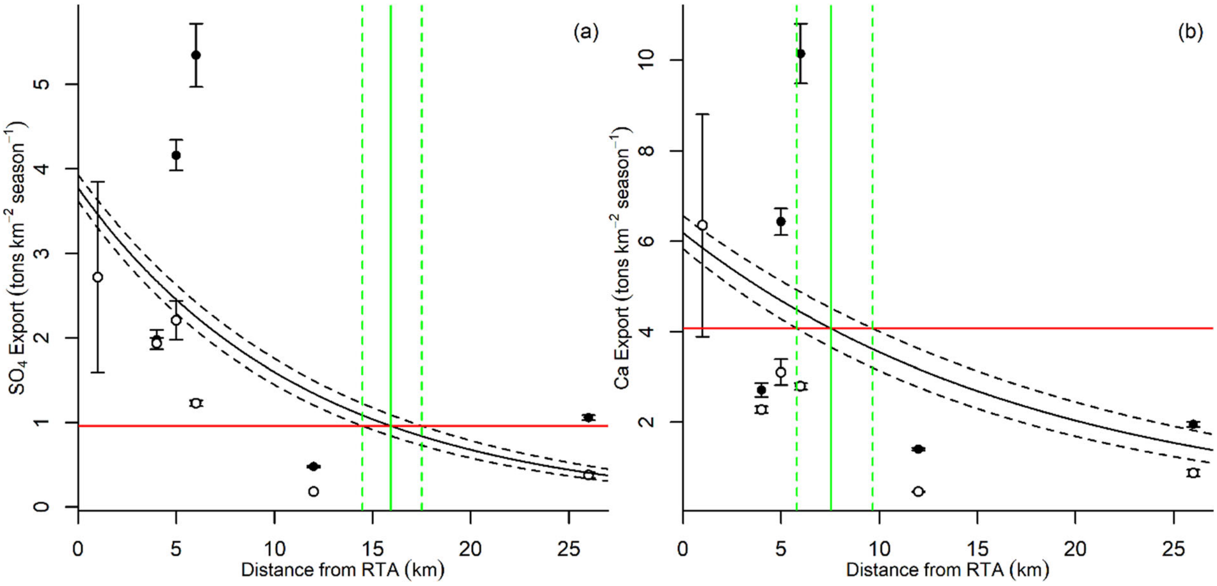

Fig. 3 **a** Sulfate (SO_4) and **b** calcium (Ca) export (tons km^{-2} $season^{-1}$) significantly increased with distance to the smokestack at the Rio Tinto Alcan (RTA) facility (points represent mean estimates of export for summer [open circles] and fall [closed circles]; error bars are standard error). Confidence intervals (CI) of 95% from a Bayesian process model of log-export as a linear function of distance are used with the median value of export from the reference watersheds (red horizontal lines) to establish what distance from the smelter (RTA) is influenced by emissions (vertical green lines). SO_4 impact distance is estimated to be 16 km (95% CI between 14 and 18 km, log(export) = 1.33 – 0.09 × distance. Ca impact distance is estimated to be 8 km (95% CI between 6 and 10 km, log(export) = 1.82 – 0.06 × distance). watersheds (circles) are in order of increasing distance from the smelter and correspond to sites # 1–6 (Fig. 1). Reference watersheds (red line) correspond to sites # 7–9 (Fig. 1; Appendix A Table S1 and S2)

2016). Critical acid load models predict that increasing S deposition may exceed soil acid buffering capacity in an area that could range from 1-28 km^2 near the smelter (Williston et al. 2016). However, data for critical acid load estimates and weathering rates (ESSA Technologies et al. 2013; 2014) lacked spatial resolution to explain our observed pattern in export. Increased export of Ca (but not other cations) was observed in impacted watersheds of both major geological types in our study. Our observed direct and indirect impacts of deposition on watershed export are similar in scale to biomonitoring studies that have detected the influence of smelter emissions on pine needle composition and moss tissues in the Kitimat valley (Cowden and Aherne 2019; Kalugina et al. 2017). Our results indicate increased Ca export associated with proximity to the smelter emissions, while base cations (Mg, K, and Na) with weaker pH-dependent charge (Sparks and Donald 2017) may be impacted at scales we cannot detect or are eventually going to be subject to export in the future. Because Ca export is an indirect response to acidic deposition, the distance of impact is smaller than direct impacts to SO_4. The 8 km impact distance indicates that biological and chemical watershed processes are being altered by atmospheric emissions of ≥ 36 kg SO_4 ha^{-1} y^{-1} over an area of 45 km^2 (Fig. 1).

F export ranged from 1.24 to 418 kg km^{-2} season^{-1}. While elevated F had been identified as a potential consequence of the smelting operation in our study area (Hocking et al. 1980) and observed concentrations in the impacted sites were elevated (Fig. 2b), here our results indicate that there is not a statistically significant (p = 0.18) increase in F export closer to the smelter emission source. The decoupling of F impact in concentration and export is likely due to the magnitude of the concentrations and uncertainty in the export estimate carried over from the flow to concentrations relationship. Thus, there is a detectable difference in instantaneous F conditions via the impact of the smelter emissions; however, the data lack the spatial resolution to link impact and distance. NO_3 export from the study area varied from 0.11 to 64.3 kg km^{-2} season^{-1}, which is within the range of previously reported NO_3 exports from similar watersheds in British Columbia (Feller 1987, 2010). As with Cl and Na, NO_3 export was highest in the two watersheds adjacent to the marine inlet; however, the export did not increase with proximity toward the smelter emission source (p = 0.25). N and F emission from the smelter are concurrent with S compounds (ESSA Technologies et al. 2013, 2014) and collectively impact NO_3 and F at the tributary scale with instantaneous concentration but lack the resolution in the relationship between export and flow to delineate a larger scale impact with seasonal export and distance to the smelter.

Cl and Na fluxes varied from 10.8 to 1900 and 63.2 to 2570 kg km^{-2} season^{-1}, respectively. Renegade and Raven (Fig. 1 sites # 1 and 2, respectively) had the highest export of Cl and Na, likely a result of marine salt deposition from the adjacent marine inlet. The remainder of the sites were within the range of previously reported values for watersheds in British Columbia (Feller 1987, 2010) indicating our estimates are appropriate and impacts related to distance and SO_4 and Ca are not a spurious trend associated with distance from the ocean (Cl p = 0.32; Na p = 0.28).

S and N deposition often lead to acid pulses within tributaries with effects on benthic algae and invertebrate stream communities (Kratz et al. 1994; Wright and Schindler 1995). Further investigations on Kitimat watershed acid pulses and F pollution are being explored by the authors as these streams sustain Pacific salmon that are important for the food security of the Haisla First Nation, as well as commercial and recreational fisheries (Nesbitt and Moore 2016; Rabnett 2014). Following a major upgrade to the aluminum smelter, Rio Tinto was granted a permit by the British Columbia Provincial Government under the Environmental Management Act to increase maximum daily atmospheric SO_2 emissions from 27 to 42 tons SO_2 day^{-1} (actual annual SO_2 emissions were 18.3 tons SO_2 day^{-1} ± 3.5 SD (1982–2015) and 28.8 tons SO_2 day^{-1} ± 1.3 SD (2016–2017) (ESSA Technologies et al. 2014; Rio Tinto 2018). Thus, there may be impacts of acidification on recipient aquatic ecosystems and their biota if recent increases in emissions exceed the natural acid buffering capacity of soils and streams.

Conclusions

More than 60 years of acidic deposition have caused increases in SO_4 and Ca export across eastern North America, with commensurate impacts on recipient aquatic ecosystems. Our results suggest these processes similarly can happen in response to industrial emissions within constrained airsheds of western Canada associated with the emissions of a single industrial project. Here using innovative flow stratification and Bayesian techniques, we document that smelter emissions are associated with watershed-scale changes in dissolved ion export, likely due to both direct and indirect pathways in terrestrial and aquatic systems.

Acknowledgments Technical support was provided by the Haisla First Nation Fisheries Commission (Michael Jacobs, Brenda Bouzane, Trevor Amos, Rachael Franz, and others; Kitamaat Village, BC) and by Hidden River Environmental Management Ltd. (Mitch Drewes, Olivia Gray, Bobbi Vojtko, and others; Terrace, BC). Access to field and laboratory equipment and facilities and advice was provided by staff at the Cultus Lake Salmon Research Laboratory (Glenn Block, Kelly Malange, Garrett Lidin, Lucas Pon, Steve McDonald, David Patterson, Erland MacIsaac, and others; DFO; Cultus Lake, BC), the Kitimat River Salmon Hatchery (Markus Feldhoff, Vince Sealy, Gord Fossl, Stephen Leask, Shaun Barbosa, and others; DFO; Kitimat, BC), and the BC Ministry of Environment (BC MOE; Patrick Williston; Smithers, BC). Background data were provided by Rio Tinto Alcan and BC MOE contained in the reports by ESSA Technologies (2013, 2014). Two anonymous reviewers provided valuable insights on the manuscript.

Funding information Funding was provided by the Haisla Nation Council (Kitamaat Village, BC), Fisheries and Oceans Canada (DFO; Vancouver, BC), the Mitacs Elevate postdoctoral fellowship program (RPW), and the Natural Sciences and Engineering Research Council of Canada (NSERC) discovery grant program (SOCM).Data availabilityMaterials presented in this manuscript are available upon request from the authors.
R code and data used in this manuscript are available at Zenodo.org, doi 10.5281/zenodo.3822367.

Compliance with ethical standards

Conflict of interest The authors do not have any conflicts of interest or competing interests to declare.

References

April, R., Keller, D., & Hluchy, M. (2016). Soils and soil acidification in the Adirondack Mountains. *Adirondack Journal of Environmental Studies, 21*(1), 12.

Bates, D., Mächler, M., Bolker, B., & Walker, S. (2015). Fitting linear mixed-effects models using lme4. *Journal of Statistical Software, 67*(1), 1–48. https://doi.org/10.18637/jss.v067.i01.

Beale, E. M. L. (1962). Some uses of computers in operational research. *Industrielle Organisation, 31*(1), 27–28.

Bozdogan, H. (1987). Model selection and Akaike's information criterion (AIC): the general theory and its analytical extensions. *Psychometrika, 52*(3), 345–370.

Bunce, H. W. F. (1989). The continuing effects of aluminium smelter emissions on coniferous forest growth. *Forestry: An International Journal of Forest Research, 62*(3), 223–231.

CABIN. (2012). Field manual: wadeable streams, Canadian Aquatic Biomonitoring Network. Environment Canada, Ottawa, ON (Vol. 6). http://publications.gc.ca/collections/collection_2012/ec/En84-87-2012-eng.pdf

Carey, J. C., & Fulweiler, R. W. (2013). Watershed land use alters riverine silica cycling. *Biogeochemistry, 113*(1–3), 525–544.

Cowden, P., & Aherne, J. (2019). Assessment of atmospheric metal deposition by moss biomonitoring in a region under the influence of a long standing active aluminium smelter. *Atmospheric Environment, 201*, 84–91.

Dolan, D. M., Yui, A. K., & Geist, R. D. (1981). Evaluation of river load estimation methods for total phosphorus. *Journal of Great Lakes Research, 7*(3), 207–214.

ESSA Technologies, Aherne, J., Cheng, H., Hall, A., Henolson, A., Laurence, J., Marmorek, D., Murray, C., and Watmough, S. (2019). Sulphur Dioxide Environmental Effects Monitoring for the Kitimat Modernization Project. Detailed Terms of Reference for the 2019 Comprehensive Review. Report prepared for Rio Tinto, BC Works. 36 pp.

ESSA Technologies, Laurence, J., Limnotek, Risk Sciences International, Rio Tinto Alcan, Trent University, et al. (2013). Sulphur dioxide technical assessment report in support of the 2013 application to amend the P2-00001 multimedia permit for the Kitimat Modernization Project. Report prepared for Rio Tinto Alcan, Kitimat, B.C. 37 pp.

ESSA Technologies, Laurence, J., Risk Sciences International, Trent University, and Trinity Consultants (2014). Kitimat airshed emissions effects assessment. Report prepared for BC Ministry of Environment, Smithers, BC. 205 pp. + appendices. http://www.bcairquality.ca/airsheds/kitimat-airshed-assessment.html .

Federer, C. A., Hornbeck, J. W., Tritton, L. M., Martin, C. W., Pierce, R. S., & Smith, C. T. (1989). Long-term depletion of calcium and other nutrients in eastern US forests. *Environmental Management, 13*(5), 593–601.

Feller, M. C. (1987). The influence of acid precipitation on stream chemistry in a small forested basin in southwestern British Columbia. *Forest Hydrology and Watershed Management, 167*, 33.

Feller, M. C. (2010). Trends in precipitation and streamwater chemistry in East Creek watershed in southwestern British Columbia, 1971–2008. *Journal of Limnology*, 77–91.

Fulweiler, R. W., & Nixon, S. W. (2005). Terrestrial vegetation and the seasonal cycle of dissolved silica in a southern New England coastal river. *Biogeochemistry, 74*(1), 115–130.

Hocking, M. B., Hocking, D., & Smyth, T. A. (1980). Fluoride distribution and dispersion processes about an industrial point source in a forested coastal zone. *Water, Air, and Soil Pollution, 14*(1), 133–157.

Jeziorski, A., Tanentzap, A. J., Yan, N. D., Paterson, A. M., Palmer, M. E., Korosi, J. B., Rusak, J. A., Arts, M. T., Keller, W. B., Ingram, R., Cairns, A., & Smol, J. P. (2015). The jellification of north temperate lakes. *Proceedings of the Royal Society B: Biological Sciences, 282*(1798), 20142449.

Johnson, J. B., & Omland, K. S. (2004). Model selection in ecology and evolution. *Trends in ecology & evolution, 19*(2), 101–108.

Kalugina, O. V., Mikhailova, T. A., & Shergina, O. V. (2017). Pinus sylvestris as a bio-indicator of territory pollution from aluminum smelter emissions. *Environmental Science and Pollution Research, 24*(11), 10279–10291.

Kratz, K. W., Cooper, S. D., & Melack, J. M. (1994). Effects of single and repeated experimental acid pulses on invertebrates in a high altitude Sierra Nevada stream. *Freshwater Biology, 32*(1), 161–183.

Likens, G. E., Driscoll, C. T., & Buso, D. C. (1996a). Long-term effects of acid rain: response and recovery of a forest ecosystem. *Science*.

Likens, G., Driscoll, C. T., Buso, D. C., Mitchell, M. J., Lovett, G., Bailey, S., et al. (1996b). Soils and soil acidification in the Adirondack Mountains. *Science*.

Maguire, T. J., & Fulweiler, R. W. (2017). The fate and effect of dissolved silicon within wastewater treatment effluent. *Environmental science & technology, 51*(*13*), 7403–7411. https://doi.org/10.1021/acs.est.7b01276.

McLinden, C. A., Fioletov, V., Shephard, M. W., Krotkov, N., Li, C., Martin, R. V Martin R. V., Moran M. D., Joiner J. (2016). Space-based detection of missing sulfur dioxide sources of global air pollution. *Nature Geoscience*, *9*(7), 496, 500.

Meybeck, M. (1982). Carbon, nitrogen, and phosphorus transport by world rivers. *Am. J. Sci, 282*(4), 401–450.

Mitchell, M. J., Lovett, G., Bailey, S., Beall, F., Burns, D., Buso, D., Clair, T. A., Courchesne, F., Duchesne, L., Eimers, C., Fernandez, I., Houle, D., Jeffries, D. S., Likens, G. E., Moran, M. D., Rogers, C., Schwede, D., Shanley, J., Weathers, K. C., & Vet, R. (2011). Comparisons of watershed sulfur budgets in southeast Canada and northeast US: new approaches and implications. *Biogeochemistry, 103*(1–3), 181–207.

Myrbo, A., Swain, E. B., Johnson, N. W., Engstrom, D. R., Pastor, J., Dewey, B., Monson, P., Brenner, J., Dykhuizen Shore, M., & Peters, E. B. (2017). Increase in nutrients, mercury, and methylmercury as a consequence of elevated sulfate reduction to sulfide in experimental wetland mesocosms. *Journal of Geophysical Research: Biogeosciences, 122*(11), 2769–2785.

Nesbitt, H. K., & Moore, J. W. (2016). Species and population diversity in Pacific salmon fisheries underpin indigenous food security. *Journal of applied ecology, 53*(5), 1489–1499.

Ohrui, K., & Mitchell, M. J. (1997). Nitrogen saturation in Japanese forested watersheds. *Ecological applications, 7*(2), 391–401.

Prietzel, J., Mayer, B., & Legge, A. H. (2004). Cumulative impact of 40 years of industrial sulfur emissions on a forest soil in west-central Alberta (Canada). *Environmental pollution, 132*(1), 129–144.

Rabnett, K. (2014). *Lower Kitimat Watershed & Estuary Restoration Priorities* . (P. for H. F. & C. DFO, Ed.) *Restoration & compensation review*. Suskwa Research.

Reddy, K. R., & DeLaune, R. D. (2008). *Biogeochemistry of wetlands: science and applications* (1st ed.). Boca Raton: CRC press.

Redfield, A. C. (1958). The biological control of chemical factors in the environment. *American Scientist*, *46*(3), 230A–221.

Reid, C. R., & Watmough, S. A. (2016). Spatial patterns, trends, and the potential long-term impacts of tree harvesting on lake calcium levels in the Muskoka River Watershed, Ontario, Canada. *Canadian journal of fisheries and aquatic sciences, 73*(3), 382–393.

Rice, K. C., Scanlon, T. M., Lynch, J. A., & Cosby, B. J. (2014). Decreased atmospheric sulfur deposition across the southeastern US: when will watersheds release stored sulfate? *Environmental science & technology, 48*(17), 10071–10078.

Rio Tinto. (2018). *Environmental Report BC Works*. Kitimat BC, Canada: Rio Tinto Plc. http://www.riotinto.com/documents/2018_BC_Works_environmental_report.pdf

Schlesinger, W. H., & Bernhardt, E. S. (2013). *Biogeochemistry: an analysis of global change* (3rd ed.). Waltham: Elsevier.

Sleighter, R. L., Chin, Y.-P., Arnold, W. A., Hatcher, P. G., McCabe, A. J., McAdams, B. C., & Wallace, G. C. (2014). Evidence of incorporation of abiotic S and N into prairie wetland dissolved organic matter. *Environmental Science & Technology Letters, 1*(9), 345–350.

Sparks, & Donald, L. (2017). *Environmental Soil Chemistry*. US: Academic Press.

Tréguer, P., & De La Rocha, C. (2013). The world ocean silica cycle. *Annual Review of Marine Science, 5*, 477–501.

Vet, R., Artz, R. S., Carou, S., Shaw, M., Ro, C.-U., Aas, W., Baker, A., Bowersox, V. C., Dentener, F., Galy-Lacaux, C., Hou, A., Pienaar, J. J., Gillett, R., Forti, M. C., Gromov, S., Hara, H., Khodzher, T., Mahowald, N. M., Nickovic, S., Rao, P. S. P., & Reid, N. W. (2014). A global assessment of precipitation chemistry and deposition of sulfur, nitrogen, sea salt, base cations, organic acids, acidity and pH, and phosphorus. *Atmospheric Environment, 93*, 3–100.

Williston, P., Aherne, J., Watmough, S., Marmorek, D., Hall, A., de la Cueva Bueno, P., Murray, C., Henolson, A., & Laurence, J. A. (2016). Critical levels and loads and the regulation of industrial emissions in northwest British Columbia, Canada. *Atmospheric environment, 146*, 311–323.

Wright, R. F., & Schindler, D. W. (1995). Interaction of acid rain and global changes: effects on terrestrial and aquatic ecosystems. *Water, Air, and Soil Pollution, 85*(1), 89–99.

Yan, N. D., Mackie, G. L., & Boomer, D. (1989). Seasonal patterns in metal levels of the net plankton of three Canadian Shield lakes. *Science of the total environment, 87*, 439–461.